



Copper(II) diclofenac complexes: Synthesis, structural studies and interaction with albumins and calf-thymus DNA

Santosh Kumar^a, Raj Pal Sharma^{a,*}, Paloth Venugopalan^a, Valeria Ferretti^{b,*}, Spyros Perontsis^c, George Psomas^{c,*}

^a Department of Chemistry and Center of Advanced Studies, Panjab University, Chandigarh 160014, India

^b Center for Structural Diffraction and Department of Chemical and Pharmaceutical Sciences, University of Ferrara, via Fossato di Mortara 17-27, I-44121 Ferrara, Italy

^c Department of General and Inorganic Chemistry, Faculty of Chemistry, Aristotle University of Thessaloniki, GR-54124 Thessaloniki, Greece

ARTICLE INFO

Keywords:

Copper(II) complexes
Diclofenac
N-donor ligand
Crystal structure
Interaction with albumin
Interaction with DNA

ABSTRACT

The reaction of the copper(II) diclofenac complex $[\text{Cu}(\text{dicl})_2(\text{H}_2\text{O})_2]$ (**1**) (*dicl* = deprotonated diclofenac) with the chelating N-donor ligands ethylenediamine (*en*), propan-1,3-diamine (*pn*), unsymmetrical dimethylethylenediamine (*unsym-dmen*) and *N,N,N',N'*-tetramethylethylenediamine (*temed*) in methanol-water (4:1 v/v) yielded the novel copper(II) complexes $[\text{Cu}(\text{en})_2(\text{H}_2\text{O})_2](\text{dicl})_2 \cdot 2\text{H}_2\text{O}$ (**2**), $[\text{Cu}(\text{pn})_2(\text{H}_2\text{O})_2](\text{dicl})_2 \cdot 2\text{H}_2\text{O}$ (**3**), $[\text{Cu}(\text{unsym-dmen})_2(\text{H}_2\text{O})_2](\text{dicl})_2 \cdot 2\text{H}_2\text{O}$ (**4**) and $[\text{Cu}(\text{temed})_2(\text{H}_2\text{O})_2](\text{dicl})_2$ (**5**), respectively. All the synthesized complexes have been characterized by spectroscopic (UV–vis, FT-IR) methods. The structures of complexes **2**, **3** and **5** were unambiguously determined by single-crystal X-ray crystallography. X-ray structures of complexes clearly revealed the ionic structure of complexes **2**, **3** and the covalent structure of **5**. The geometry of complex **4** was optimized by DFT calculations. The ability of the complexes **1–5** to bind to calf-thymus DNA was monitored *in vitro* by diverse techniques (UV–vis spectroscopy, cyclic voltammetry, viscosity measurements) and *via* competitive studies with ethidium bromide. The interaction of complexes **1–5** with bovine serum albumin was studied *in vitro* by fluorescence emission spectroscopy and the corresponding binding constants were calculated. The biological behavior of complexes **1–5** was compared with previously reported Cu(II), Mn(II) and Ni(II) complexes of diclofenac.

1. Introduction

It has been more than fifty years that Prof. Rosenberg discovered the activity of *cisplatin* ($[\text{Pt}(\text{NH}_3)_2\text{Cl}_2]$) against cancer cells [1–3]. This discovery provided a boost to “medicinal inorganic chemistry” which focuses on the design and discovery of metal-based drugs not only as anticancer agents but also for any possible therapeutic applications. Nowadays, metal complexes that are examined *in vitro* for their potential activity may contain diverse transition metal ions and a variety of ligands, and their potential applications cover a wide spectrum of activities against infections, inflammations and diseases [4–6].

Many of the used anticancer drugs are DNA-damaging agents [7]. Therefore, DNA is recognized as one of the most common biological targets of anticancer drugs. In general, transition metal

complexes may bind to double-stranded DNA mainly in three fashions: (a) *via* covalent binding, *i.e.* replacement of a labile ligand of the complex by a nitrogenous DNA-base, (b) through noncovalent interactions, *i.e.* intercalation *via* $\pi \rightarrow \pi$ stacking of the complex in-between DNA-bases, electrostatic interactions resulting from Coulomb forces between metal complexes and the phosphate groups of DNA, and groove-binding occurring along major or minor groove of DNA helix upon the development of van der Waals forces or hydrogen-bonding or hydrophobic bonding and (c) cleavage of the DNA double-stranded helix may occur along and/or across the strands [8–12].

The pioneering work of Sorenson provided a tremendous boost to research on copper(II) complexes for exploring their potential biological activity [13]. Copper is among the most abundant transition metals in the human body and plays several roles in human

* Corresponding authors.

Email addresses: rpsharmapu@yahoo.co.in (R.P. Sharma); frt@unife.it (V. Ferretti); gepsomas@chem.auth.gr (G. Psomas)

physiology and is involved in the active center of enzymes responsible for numerous redox processes while its excess or deficiency may cause diseases, such as Wilson's disease or Menkes syndrome [14,15]. As a result of its bacteriostatic activity, copper is used for the manufacturing of touch surfaces in hospitals and healthcare settings [16]. The mixture of ternary Cu(II) complexes called "Casiopinas®" is in clinical trials for its cytostatic, cytotoxic and anti-neoplastic activities [17]. Copper(II) complexes are attractive as metal-based drugs because: (i) Cu(II) salts as starting material are cheaper than other metal salts, making treatment more affordable for the poor, (ii) the copper(II) complexes of several drugs (antibacterial [18], antifungal [19], anti-inflammatory [20], antiviral [21] agents) as ligands are more active than the parent drugs [22] and (iii) the biological activity of copper(II) complexes with nitrogen-donor ligands have been found to be higher than the original ligands [14,23–25]. In the context of medicinal inorganic chemistry, copper(II) complexes have shown noteworthy *in vitro* biological activity including anticancer [26], antifungal [27], anti-inflammatory [28], antimicrobial [29] and antioxidant [30] activity.

Non-steroidal anti-inflammatory drugs (NSAIDs) constitute a commercially important class of drugs to cure pain and inflammation associated with diseases or injuries, including intestinal disease and migraine [31]. Furthermore, the mechanisms of action of the anti-tumorigenic effects of NSAIDs have not been yet completely revealed and may include COX-independent mechanisms, apoptosis, free radical involvement or other unknown molecular mechanisms [32–34]. Within this context, the interaction of NSAIDs with DNA (which is also a biological target for anticancer drugs) is of great interest in order to try to explain the potential anticancer and antiinflammatory activities [35,36]. Moreover, from a metal-complexes synthetic point of view, the carboxylic NSAIDs (*i.e.* salicylate derivatives, phenylalkanoic acids, and anthranilic acids) are particularly interesting since their carboxylic group –COOH may exhibit upon deprotonation a variety of coordination modes towards metal ions, *e.g.* monodentate, bidentate, bidentate chelating or bidentate bridging [37].

Diclofenac (*Hdicl*) (Fig. 1(a)) is a widely used anti-inflammatory, analgesic and antipyretic agent. Sodium diclofenac (*Nadicl*) is NSAID phenylalkanoic acid derivative used in the treatment of rheumatoid arthritis and osteoarthritis [38–41]. As for its metal complexes reported in the literature, the copper [41–44], manganese [45–47], cadmium [48], tin [49] and nickel [50] complexes have been studied.

In view to our long experience in structural chemistry of copper(II) carboxylates [51–56], we started a research program aiming at the synthesis and characterization of copper(II) complexes of NSAIDs, evaluating their ability to interact with DNA and albumins and possibly assessing their structure-activity relationship [30,42,44,57–68]. The characteristic features of our methodology are: (i) cheap and readily available starting materials, (ii) simple and convenient synthesis at room temperature, (iii) nearly quantitative yields. The understanding of the modes of action of potential metal-based drugs necessitates the study of interaction with possible biological targets including aminoacids, proteins, and biological

macromolecules [69]. The study of the interaction with the potential biological target DNA as well as with the drug-carrier protein albumin is a first approach for further therapeutic applications.

As a continuation of our research project regarding the synthesis and biological evaluation of copper(II)/N-donor ligands [51–58], we report herein, the synthesis and characterization of four new copper(II)-diclofenac complexes in presence of the N-donor ligands, such as ethylenediamine (*en*), propan-1,3-diamine (*pn*), unsymmetrical dimethylethylene-diamine (*unsym-dmen*) and *N,N,N',N'*-tetramethylethylenediamine (*temed*) (Fig. 1(b)–(e)), namely, $[\text{Cu}(\text{en})_2(\text{H}_2\text{O})_2](\text{dicl})_2 \cdot 2\text{H}_2\text{O}$ (2), $[\text{Cu}(\text{pn})_2(\text{H}_2\text{O})_2](\text{dicl})_2 \cdot 2\text{H}_2\text{O}$ (3), $[\text{Cu}(\text{unsym-dmen})_2(\text{H}_2\text{O})_2](\text{dicl})_2 \cdot 2\text{H}_2\text{O}$ (4) and $[\text{Cu}(\text{temed})(\text{dicl})_2]$ (5), along with previously reported $[\text{Cu}(\text{dicl})_2(\text{H}_2\text{O})_2]$ (1) [58]. The *in vitro* biological activities of the resultant complexes have been also considered. More specifically, as a first approach for the potential use of the complexes as metallopharmaceutical agents, their *in vitro* affinity for bovine serum albumin (BSA) has been monitored by fluorescence emission spectroscopy and their *in vitro* interaction with calf-thymus (CT) DNA has been examined by UV–visible (UV–vis) spectroscopy, viscosity measurements, cyclic voltammetry and *via* their ability to displace ethidium bromide (EB) from the EB-DNA conjugate (which has been studied by fluorescence emission spectroscopy).

2. Experimental

2.1. Materials and physical measurements

Nadicl, $\text{CuSO}_4 \cdot 5\text{H}_2\text{O}$, CT DNA, BSA, EB, NaCl and trisodium citrate were purchased from Sigma-Aldrich Co and all solvents were purchased from Merck. All chemicals and solvents were reagent grade and were used as purchased without any further purification. DNA stock solution was prepared by dilution of CT DNA to buffer (containing 15 mM trisodium citrate and 150 mM NaCl at pH 7.0) followed by vigorous stirring for three days, and kept at 4 °C for no longer than a week. This solution of CT DNA gave a ratio of UV absorbance at 260 and 280 nm (A_{260}/A_{280}) of 1.87, indicating that the DNA was sufficiently free of protein contamination [70]. The DNA concentration was determined by the UV absorbance at 260 nm after 1:20 dilution using $\epsilon = 6600 \text{ M}^{-1} \text{ cm}^{-1}$ [71].

Elemental analysis was performed using an automatic Perkin Elmer 2400 CHN element analyzer and copper content was gravimetrically determined as CuSCN by standard literature methods [72]. Attenuated Total Reflection-Fourier transform infrared spectra (ATR-FT-IR) were recorded on Perkin Elmer Spectrum RX FT-IR spectrometer (symbols used denote: m = medium, s = strong, w = weak). The UV–vis spectra of the complexes were recorded on a Hitachi U-2001 dual beam spectrophotometer using DMSO:water as solvent. The molar conductivity measurements were performed on 1 mM DMSO solution of the complexes with a Crison Basic 30 conductometer. The fluorescence spectra of all complexes 1–5 were recorded in solution on a Hitachi F-7000 fluorescence spectrophotometer. The viscosity experiments were carried out using an ALPHA L Fungilab rotational viscometer equipped with an 18-mL LCP spindle and the measurements were performed

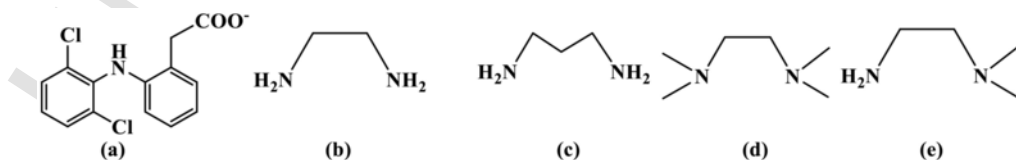


Fig. 1. Ligands used in this work: (a) diclofenac anion (*dicl*[−]), (b) ethylenediamine (*en*), (c) propan-1,3-diamine (*pn*), (d) *N,N,N',N'*-tetramethylethylenediamine (*temed*) and (e) unsymmetrical dimethylethylenediamine (*unsym-dmen*).

at 100 rpm. Cyclic voltammetry studies were performed on an Eco Chemie Autolab Potentiostat and the experiments were performed on a 30 mL three-electrode electrolytic cell. The working electrode was platinum disk. A separate Pt single-sheet electrode was used as the counter electrode and a Ag/AgCl electrode saturated with KCl was used as the reference electrode. Oxygen was removed by purging the solutions with pure nitrogen. All electrochemical measurements were performed at $25.0 \pm 0.2^\circ\text{C}$.

2.2. Preparation of complexes

2.2.1. Synthesis of $[\text{Cu}(\text{dicl})_2(\text{H}_2\text{O})_2]$, 1

$\text{CuSO}_4 \cdot 5\text{H}_2\text{O}$ (0.50 g, 2 mmol) was dissolved in 10 mL of distilled water and sodium diclofenac (1.27 g, 4 mmol) was also dissolved in minimum amount of water. On mixing the two solutions, a light-green precipitate of hydrated copper(II) diclofenac was formed immediately which was filtered through a fine filter paper, washed with water followed by methanol and dried at room temperature (yield 90%, 1.24 g). Complex 1 is insoluble in water but soluble in organic solvents like methanol, chloroform, DMSO. ATR-FT-IR (cm^{-1}): 3420(m), 3290(s), 2159(w), 1554(s), 1496(s), 1453(s), 1339(s), 1303(w), 1202(s), 1088(s), 945(m), 872(w), 535(s); $\Delta\nu(\text{COO})_{\text{dicl}} = \nu_{\text{asym}}(\text{COO})_{\text{dicl}} - \nu_{\text{sym}}(\text{COO})_{\text{dicl}} = 215 \text{ cm}^{-1}$. UV-vis (DMSO-water), λ_{max} (nm) (ϵ , in $\text{M}^{-1} \text{ cm}^{-1}$): 752 (120). Anal. Cal. for $\text{C}_{28}\text{H}_{24}\text{N}_2\text{O}_6\text{CuCl}_4$ (MW = 689.50): C, 48.73; H, 3.48, N, 4.06; Cu, 9.20%; found: C, 48.55; H, 3.55; N, 4.25; Cu, 9.02%. Molar conductivity in 1 mM DMSO solution, $\Lambda_{\text{M}} = 7 \text{ S cm}^2 \text{ mol}^{-1}$.

2.2.2. Synthesis of $[\text{Cu}(\text{en})_2(\text{H}_2\text{O})_2](\text{dicl})_2 \cdot 2\text{H}_2\text{O}$, 2

Complex 2 was synthesized from complex 1. 0.5 g (0.07 mmol) of complex 1 was dissolved in methanol:water (4:1 v/v) and *en* (in excess) was added slowly under stirring until a clear violet solution appeared. When the reaction mixture was allowed to evaporate slowly at room temperature, violet crystals appeared after a few days, which were separated from the mother liquor and dried in air. Complex 2 (yield 82%, 0.50 g) is soluble in water and DMSO, insoluble in methanol, acetone and decomposes at 184°C . ATR-FT-IR (cm^{-1}): 3234(s), 2968(m), 1608(m), 1577(s), 1552(s), 1496(m), 1451(m), 1379(s), 1291(w), 1154(s), 1083(m), 839(m), 530(s), 469(s); $\Delta\nu(\text{COO}) = 198 \text{ cm}^{-1}$. UV-vis (DMSO-water), λ_{max} (nm) (ϵ , in $\text{M}^{-1} \text{ cm}^{-1}$): 575 (58). Anal. Cal. for $\text{C}_{32}\text{H}_{44}\text{Cl}_2\text{N}_6\text{O}_8\text{Cu}$ (MW = 846.07): C, 45.38; H, 5.20, N, 9.92; Cu, 7.50%; found: C, 45.28; H, 5.32; N, 10.01; Cu, 7.61%. Molar conductivity in 1 mM DMSO solution, $\Lambda_{\text{M}} = 30 \text{ S cm}^2 \text{ mol}^{-1}$.

2.2.3. Synthesis of $[\text{Cu}(\text{pn})_2(\text{H}_2\text{O})_2](\text{dicl})_2 \cdot 2\text{H}_2\text{O}$, 3

Complex 3 was synthesized in a similar manner as complex 2 by adding *pn* (in excess) instead of *en* until a clear blue-colored solution was obtained. When the reaction mixture was allowed to evaporate slowly at room temperature, blue crystals appeared after four days, which were separated from the mother liquor and dried in air. Complex 3 (yield 78%, 0.47 g) is also soluble in water and DMSO, insoluble in methanol and decomposes at 172°C . ATR-FT-IR (cm^{-1}): 3366(s), 3240(s), 2985(m), 1634(w), 1549(s), 1492(s), 1377(s), 1156(s), 921(w), 743(w), 583(w), 532(s), 457(m); $\Delta\nu(\text{COO}) = 172 \text{ cm}^{-1}$. UV-vis (DMSO-water), λ_{max} (nm) (ϵ , in $\text{M}^{-1} \text{ cm}^{-1}$): 560 (162). Anal. Cal. for $\text{C}_{34}\text{H}_{48}\text{Cl}_2\text{N}_6\text{O}_8\text{Cu}$ (MW = 874.12): C, 46.67; H, 5.49, N, 9.60; Cu, 7.26%; found: C, 46.72; H, 5.40; N, 9.72; Cu, 7.18%. Molar conductivity in 1 mM DMSO solution, $\Lambda_{\text{M}} = 35 \text{ S cm}^2 \text{ mol}^{-1}$.

2.2.4. Synthesis of $[\text{Cu}(\text{unsym-dmen})_2(\text{H}_2\text{O})](\text{dicl})_2 \cdot \text{H}_2\text{O}$, 4

Complex 4 was synthesized in a similar manner as complex 2 by adding *unsym-dmen* (in excess) in place of *en* until a clear blue-col-

ored solution was obtained. When the reaction mixture solution was allowed to evaporate slowly at room temperature, blue crystals appeared after three days, which were separated from the mother liquor and dried in air. Complex 4 (yield 85%, 0.53 g) is also soluble in water and DMSO and insoluble in methanol and decomposes at 175°C . ATR-FT-IR (cm^{-1}): 3153(s), 3087(m), 2962(w), 2843(w), 1573(s), 1552(m), 1360(s), 1146(s), 1042(m), 780(s), 742(s), 546(s), 525(s), 455(s); $\Delta\nu(\text{COO}) = 213 \text{ cm}^{-1}$. UV-vis (DMSO-water), λ_{max} (nm) (ϵ in $\text{M}^{-1} \text{ cm}^{-1}$): 563 (188). Anal. Cal. for $\text{C}_{38}\text{H}_{48}\text{Cl}_4\text{CuN}_6\text{O}_6$ (MW = 866.04): C, 49.88; H, 4.67, N, 9.69; Cu, 7.73%; found: C, 50.10; H, 4.60; N, 9.75; Cu, 7.62%. Molar conductivity in 1 mM DMSO solution, $\Lambda_{\text{M}} = 40 \text{ S cm}^2 \text{ mol}^{-1}$.

2.2.5. Synthesis of $[\text{Cu}(\text{tmed})_2(\text{dicl})_2]$, 5

Complex 5 was synthesized in a similar manner as complex 2 by adding *tmed* (in excess) in place of *en* until a clear royal-blue solution was obtained. When the reaction mixture solution was allowed to evaporate slowly at room temperature, royal-blue crystals appeared after a few days, which were separated from the mother liquor and dried in air. Complex 5 (yield 88%, 0.49 g) is also insoluble in water and soluble in methanol, DMSO and other organic solvents and decomposes at 210°C . ATR-FT-IR (cm^{-1}): 3214(s), 2990(m), 1615(m), 1573(s), 1496(m), 1334(s), 1146(s), 950(s), 868(m), 746(s), 658(s), 555(s), 520(s), 470(s); $\Delta\nu(\text{COO}) = 239 \text{ cm}^{-1}$. UV-vis (DMSO-water), λ_{max} (nm) (ϵ in $\text{M}^{-1} \text{ cm}^{-1}$): 662 (108). Anal. Cal. for $\text{C}_{34}\text{H}_{36}\text{Cl}_4\text{CuN}_4\text{O}_4$ (MW = 770.01): C, 52.98; H, 4.67, N, 7.27; Cu, 8.24%; found: C, 53.10; H, 4.54; N, 7.32; Cu, 8.15%. Molar conductivity in 1 mM DMSO solution, $\Lambda_{\text{M}} = 5 \text{ S cm}^2 \text{ mol}^{-1}$.

2.3. Albumin and DNA-binding studies

In order to evaluate the biological behavior of complexes 1–5, the compounds were initially dissolved in DMSO (1 mM). Mixing of such solutions with the aqueous buffer DNA/BSA-containing solutions used in the studies never exceeded 5% DMSO (v/v) in the final solution, which was needed due to low aqueous solubility of most complexes. All studies were performed at room temperature. The biological behavior of free sodium diclofenac was previously reported [42]. Control experiments with DMSO were performed and no changes in the spectra of BSA or CT DNA were observed.

2.3.1. BSA-binding studies

The albumin binding studies were performed by performing tryptophan fluorescence quenching experiments using BSA (3 μM) in buffer (15 mM trisodium citrate and 150 mM NaCl at pH 7.0). The quenching of the emission intensity of tryptophan residues of BSA at 342 nm was monitored using complexes 1–5 as quenchers with gradually increasing concentration and the fluorescence emission spectra were recorded in the range of 300–500 nm with excitation wavelength of 295 nm [73]. Complexes 1–5 exhibited in buffer solution two low-intensity emission bands at ~ 349 and ~ 362 nm, when the fluorescence emission spectra were recorded under the same experimental conditions, i.e. excitation at 295 nm [42]. Therefore, the quantitative studies of the BSA fluorescence spectra were performed after their correction by subtracting the spectra of the complexes. The influence of the inner-filter effect [74] on the measurements was evaluated by eq. S1; it was too low and did not affect the measurements. The Stern-Volmer and Scatchard equations (eqs. S2–S4) [75] and graphs were used in order to study the interaction of each complex-quencher with BSA and calculate the Stern-Volmer constant K_{SV} (in M^{-1}), the quenching constant k_q (in $\text{M}^{-1} \text{ s}^{-1}$), the BSA-binding constant K (in M^{-1}) and the number of binding sites per albumin.

2.3.2. DNA-binding studies

The investigation of the possible binding modes of complexes 1–5 to CT DNA and the calculation of the corresponding DNA-binding constants (K_b) were carried out by UV–vis spectroscopy. The UV–vis spectra of a solution of CT DNA ($1.2\text{--}1.4 \times 10^{-4}\text{M}$) were recorded in the presence of each complex at diverse [complex]/[DNA] mixing ratios ($=r$). The DNA-binding constants of the complexes, K_b (in M^{-1}), were determined by the Wolfe-Shimer equation (eq. S5) [76] and the plots $[\text{DNA}]/(\epsilon_A - \epsilon_f)$ versus [DNA] using the UV–vis spectra of the complexes ($1.5 \times 10^{-5}\text{M}$) recorded in the presence of DNA at increasing concentrations.

The viscosity of DNA ([DNA] = 0.1 mM) in buffer solution (150 mM NaCl and 15 mM trisodium citrate at pH 7.0) was measured in the presence of increasing amounts of complexes 1–5 (up to $r = 0.36$). All measurements were performed at room temperature and the obtained data are presented as $(\eta/\eta_0)^{1/3}$ versus r , where η is the viscosity of DNA in the presence of the complex, and η_0 is the viscosity of free DNA in buffer solution.

The interaction of complexes 1–5 with CT DNA was also investigated via monitoring the changes observed in the cyclic voltammogram of a 0.40 mM 1:2 DMSO:buffer solution of complex upon addition of DNA solution at diverse r values. The buffer was also used as the supporting electrolyte and the cyclic voltammograms were recorded at $\nu = 100\text{ mVs}^{-1}$. The ratio of the DNA-binding constants for the reduced form (K_r) and oxidized forms (K_{ox}) of the complexes (K_r/K_{ox}) was calculated according to eq. S6 [77].

Fluorescence emission spectroscopy was applied in order to examine whether each complex may compete with EB for the DNA-intercalating sites by displacing it from its DNA-EB conjugate. The DNA-EB conjugate was prepared by adding 20 μM EB and 26 μM CT DNA in buffer solution (150 mM NaCl and 15 mM trisodium citrate at pH 7.0). The possible intercalating effect of the complexes was studied by the stepwise addition of a certain amount of a compound's solution into a solution of the DNA-EB conjugate. The resultant changes were observed by recording the variation of fluorescence emission spectra with excitation wavelength at 540 nm. Complexes 1–5 do not show any appreciable fluorescence emission bands at room temperature in solution or in the presence of DNA or EB under the same experimental conditions, i.e.

$\lambda_{\text{excitation}} = 540\text{ nm}$; therefore, the observed quenching is attributed to the displacement of EB from its EB-DNA conjugate. The values of the Stern-Volmer constant (K_{SV} , in M^{-1}) were calculated according to the linear Stern-Volmer equation (eq. S2) [78] and the plots I_0/I versus $[Q]$. Taking $\tau_0 = 23\text{ ns}$ as the fluorescence lifetime of the EB-DNA system [79], the quenching constants (k_q , in $\text{M}^{-1}\text{s}^{-1}$) for the complexes were calculated according to eq. S3.

2.4. X-ray crystallography

The crystallographic data for complexes 2, 3 and 5 were collected on a Nonius Kappa CCD diffractometer at room temperature using graphite-monochromated Mo-K α radiation ($\lambda = 0.71073\text{ \AA}$) with a φ scan followed by ω scan to fill the sphere. All intensities were corrected for Lorentz, polarization and absorption effects [80]. The structures were solved by direct methods with the SIR97 program [81] and refined on F^2 by full-matrix least-squares methods with anisotropic non-H atoms. The hydrogen atoms linked to the diclofenac nitrogen in all the three compounds, and those belonging to water molecules in complex 3, were found in the Difference Fourier map and refined isotropically. The hydrogen atoms of the water molecules in complex 2 were located in the difference Fourier map and their coordinates were kept fixed during the refinement. All other hydrogen atoms were included on calculated positions, riding on their carrier atoms. All other calculations were accomplished using SHELXL-2014/7 [82] and WingX [83]. Crystal data of all complexes 2, 3 and 5 are given in Table 1.

2.5. DFT calculations

The geometry of cation $[\text{Cu}(\text{unsym-dmen})_2(\text{H}_2\text{O})_2]^{2+}$ in complex 4 was optimized *in vacuum* without any symmetry constraints, starting from an octahedral geometry with the two water molecules in apical position. Calculations were carried out with the Gaussian09 suite of programs [84] employing the B3LYP [85,86] functional in combination with a LANL2DZ [87] basis set for copper and a 6-311G(d,p) basis set for the remaining atoms. Moreover, to evaluate the effects of solvation, calculations were repeated using a continuum solvation model [88] for water.

Table 1
Crystal data, experimental details, refinement details of complexes 2, 3 and 5.

	2	3	5
Crystal data			
Chemical formula	$2(\text{C}_{14}\text{H}_{10}\text{Cl}_2\text{NO}_2) \cdot \text{C}_4\text{H}_{20}\text{CuN}_4\text{O}_2 \cdot 2(\text{H}_2\text{O})$	$2(\text{C}_{14}\text{H}_{10}\text{Cl}_2\text{NO}_2) \cdot \text{C}_6\text{H}_{24}\text{CuN}_4\text{O}_2 \cdot 2(\text{H}_2\text{O})$	$\text{C}_{34}\text{H}_{36}\text{Cl}_4\text{CuN}_4\text{O}_4$
M_r	846.07	874.12	770.01
Crystal system, space group	Monoclinic, $P2_1/c$	Monoclinic, $P2_1/c$	Monoclinic, $C2/c$
a (\AA)	20.4114 (4)	20.8353 (2)	27.3412 (6)
b (\AA)	9.4627 (2)	9.6328 (3)	7.9522 (2)
c (\AA)	9.9088 (9)	9.8833 (7)	16.3311 (5)
β ($^\circ$)	99.9530 (16)	100.042 (2)	95.8760 (9)
V (\AA^3)	1885.05 (18)	1953.21 (15)	3532.09 (16)
Z	2	2	4
Radiation type	Mo $K\alpha$	Mo $K\alpha$	Mo $K\alpha$
μ (mm^{-1})	0.92	0.89	0.96
Crystal size (mm)	$0.60 \times 0.53 \times 0.15$	$0.47 \times 0.17 \times 0.15$	$0.18 \times 0.12 \times 0.10$
No. of reflections: measured, independent and observed [$I > 2\sigma(I)$]	10,764, 4482, 3422	15,159, 4685, 3608	16,605, 4258, 3012
R_{int}	0.040	0.045	0.054
$R[F^2 > 2\sigma(F^2)]$, $wR(F^2)$, S	0.046, 0.133, 1.07	0.044, 0.126, 1.09	0.046, 0.116, 1.02
No. of reflections	4482	4685	4258
No. of parameters	240	265	261
$\Delta\rho_{\text{max}}$, $\Delta\rho_{\text{min}}$ (e \AA^{-3})	0.78, -0.49	0.50, -0.47	0.43, -0.46

3. Results and discussion

3.1. Synthesis

The hydrated copper(II)-diclofenac complex **1** [39] was obtained by reacting hydrated copper sulfate with sodium salt of diclofenac as shown in Scheme 1 (eq. (i)). The precipitated product (complex **1**) was then suspended in methanol-water mixture (4:1, v/v) followed by the addition of the corresponding nitrogen-donor ligands (*en*, *pn*, *unsym-dmen*, *temed*) with continuous stirring until a clear solution was observed in each case. Upon slow evaporation of respective resultant reaction mixtures at room temperature, five complexes **1–5** were isolated in good yield (yields of all complexes **1–5** were mentioned in Experimental section) from the respective solutions as shown in Scheme 1.

The composition of each complex was indicated by elemental analyses. The mode of coordination of carboxylate group in the diclofenac ligand and possible geometry of complex was suggested by spectroscopic methods (ATR-FT-IR and UV-vis). The exact structures of complexes **2**, **3** and **5** were unambiguously established by single crystal X-ray structure determination. The structure of complex **4** was optimized by DFT calculations.

3.2. Structure of the complexes

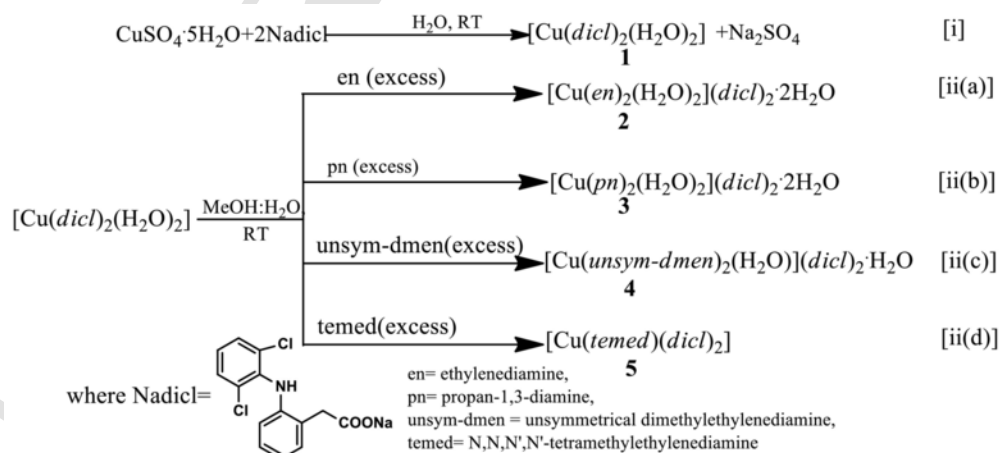
Although it was believed earlier that copper(II) diclofenac complex, **1** is dimeric in nature like other monohydrated copper(II) arylcarboxylates, its recently published X-ray structure revealed it to be monomeric having CuO₄ chromophore [58]. The ORTEP view [89] of complexes **2**, **3** and **5** are shown in Figs. 2 and 3 and selected bond distances and angles are cited in Table 2. Complexes **2** and **3** have similar structures. In both structures, the central copper atom lies on a symmetry center; the coordination geometry is elongated octahedral, with two aqua ligands occupying the apical positions, while the diclofenac anionic moieties are located outside the first coordination sphere. The asymmetric unit is completed by a solvate water molecule (Fig. 2). Conversely, in the structure of **5** (Fig. 3) the Cu atom is located on a twofold axis and it is bound to two diclofenac ligands and one *temed* ligand; the diclofenac acts as a bidentate ligand coordinated *via* the carboxylate group, with different Cu—O distances (Table 2), since the one is much longer than the other. The resulting geometry is highly distorted octahedral.

In all complexes, the Cu—N distances are very similar, as ex-

pected due to the chemical similarity of the chelating ligands. As for the Cu—O_(carboxylate) distances, their histogram obtained by searching Cu/benzoate derivatives in the Cambridge Crystallographic Database shows a clearly bimodal distribution, with maxima at around 1.99 and 2.60 Å, in good agreement with what found in complex **5**.

As for the Cu complex **4** containing *unsym-dmen* ligand, it was not possible to obtain crystals suitable for X-Ray diffraction analysis; however, the complex characterization (*vide supra*) is consistent with the presence of a [Cu(*unsym-dmen*)₂(H₂O)₂]²⁺ or [Cu(*unsym-dmen*)₂(H₂O)]²⁺ cations. DFT calculations were carried out starting from the octahedral geometry and gave as a result the square pyramidal geometry shown in Fig. 4, where one of the apical water molecules is located 3.8 Å far from the central metal. The atomic coordinates of the *in vacuo* optimized geometry are listed in Table S1 of the supplementary material. When the calculations were repeated in simulated solvent (water), it was not possible to reach a convergence because the connection between the pyramidal complex and one of the apical water molecules was completely lost. Moreover, a search of Cu(II) (*N,N*-dimethyl/diethyl-ethylenediamine) aqua-complexes in the Cambridge Crystallographic Database pointed out that, out of six structures found, only in one case the complex geometry is octahedral with two apical water molecules [90]. Even if not conclusive, these findings lead us to consider the square pyramidal geometry as the most likely.

Due to the aforementioned structural similarity, complexes **2** and **3** exhibit also a very similar packing pattern (Fig. S1). The main and strongest interactions are of O—H...O type, and involve the carboxylate oxygen atoms and the water molecules, both coordinated and free (Table S2); the O...O distances vary in the range 2.667(4)–2.745(3) Å and 2.710(3)–2.762(3) Å for **2** and **3**, respectively, and are typical of medium-to-strong hydrogen bonds. In both structures, each Cu complex is surrounded by six anionic moieties and two water molecules, as shown in Fig. 5 for **2**; two of them are directly linked to the copper complex moiety, one oxygen of the carboxylate group acting as H-bonding acceptor from the bound water molecule, while in the other cases the co-crystallized free water molecules have the task of bridging anions and cations. In contrast, N—H...O interactions are definitely weaker, with N... distances > 3 Å, with the exception of the intramolecular N3—H...O hydrogen bond present in the diclofenac molecule. As for the structure of complex **5**, besides the usual intramolecular N—H...O bond, no other significant interactions have been found.



Scheme 1. Schematic representation of synthesis of complexes **1–5**.

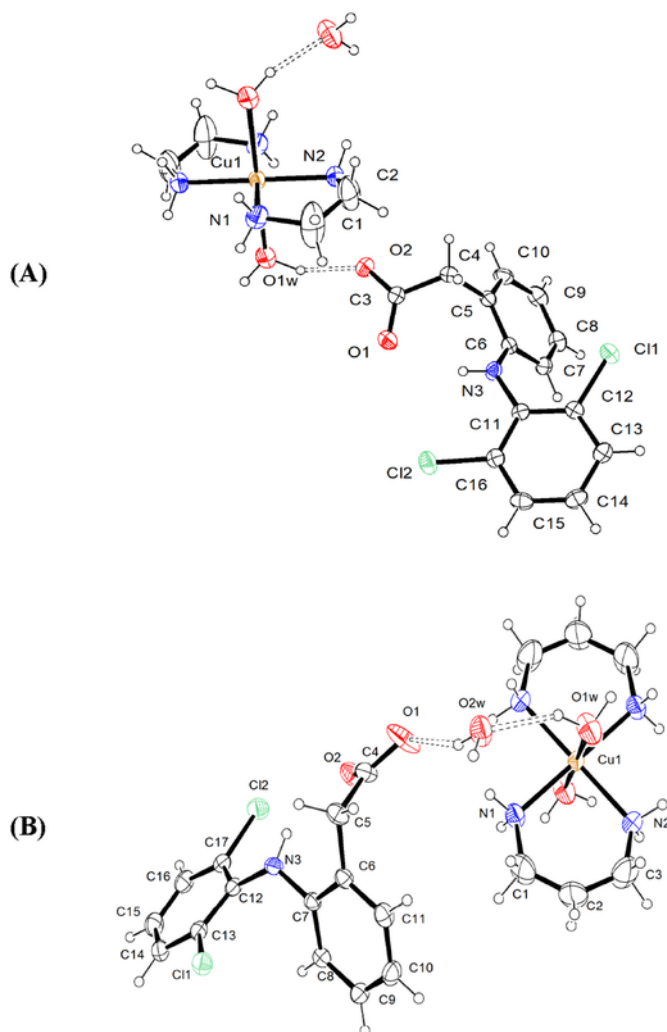


Fig. 2. ORTEP view and atom numbering scheme of complexes (A) 2 and (B) 3. Thermal ellipsoids are drawn at the 40% probability level. Hydrogen bonds are drawn as dashed lines.

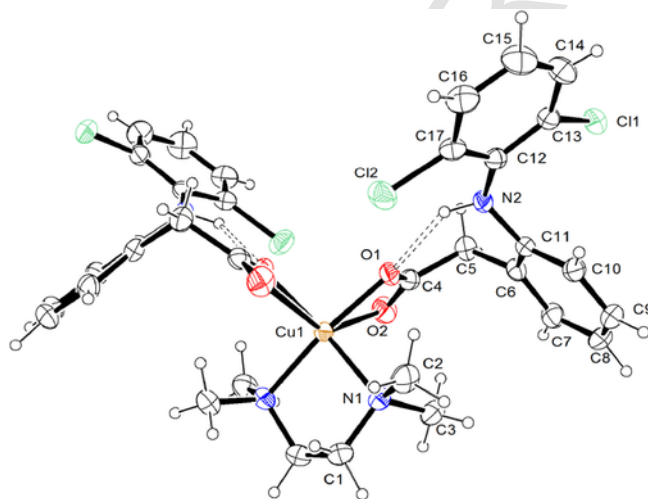


Fig. 3. ORTEP view and atom numbering scheme of complex 5. Thermal ellipsoids are drawn at the 40% probability level. Hydrogen bonds are drawn as dashed lines.

3.3. Spectroscopic characterization

FT-IR spectra of complexes 1–5 were recorded in the region 4000–400 cm^{-1} and tentative band assignment has been made on the basis of earlier reports in literature [91–94]. In solid state IR spectra of complexes 1–4, significant broad peaks were observed in the region 3500–3300 cm^{-1} indicating the stretching vibration of O—H of water molecule in these complexes. The sharp peaks in the region 3300–3100 cm^{-1} in the FT-IR spectra of the complexes indicated —N—H stretching frequency of diclofenac molecule. The peaks observed in the region 3100–2900 cm^{-1} were assigned to C(sp²)—H stretching vibration of diclofenac moieties in all complexes. The sharp peaks appeared in the region 1612–1575 cm^{-1} and 1395–1350 cm^{-1} corresponding to the antisymmetric, $\nu_{\text{asym}}(\text{COO})$, and symmetric, $\nu_{\text{sym}}(\text{COO})$, stretching vibrations of carboxylate group of diclofenac [91–94]. The parameter $\Delta\nu(\text{COO})$ ($=\nu_{\text{asym}}(\text{COO})-\nu_{\text{sym}}(\text{COO})$) can be used as important tool in assigning the mode of coordination of carboxylate ligand in metal-carboxylate complexes. From various coordination modes of carboxylate coordination, i) ionic, ii) monodentate, iii) bidentate chelating and iv) bidentate bridging are the most common ones. In complexes 2–4, the $\Delta\nu(\text{COO})$ values lie in the range 220–160 cm^{-1} observed for ionic complexes, e.g. sodium formate ($\Delta\nu(\text{COO}) = 201 \text{ cm}^{-1}$), sodium acetate ($\Delta\nu(\text{COO}) = 164 \text{ cm}^{-1}$), sodium ibuprofen ($\Delta\nu(\text{COO}) = 190 \text{ cm}^{-1}$) and sodium diclofenac ($\Delta\nu(\text{COO}) = 170 \text{ cm}^{-1}$) [95]. For complexes 1 and 5, the higher value of $\Delta\nu(\text{COO})$, i.e. above 220 cm^{-1} , indicated the covalent nature of these complexes and the monodentate binding mode of the carboxylate group of diclofenac ligands. The peaks observed in the region 1000–620 cm^{-1} might be assigned to in-plane bending and out-of-plane deformation vibrations of hydrogen atoms on aromatic rings. The peaks observed around 500 cm^{-1} in complexes 1–5 are within the range reported for Cu—O and Cu—N stretching frequencies in the literature. The FT-IR spectra for complexes 1–5 are shown in Fig. S2.

Although electronic spectroscopy is a useful technique to predict geometry of a transition metal ion in a metal complex, it is difficult sometimes to predict exact geometry of a copper(II) complex mainly due to various geometries possible in case of copper in the +2 oxidation state only. However detailed analyses of X-ray structures and solid or solution state electronic spectra of copper(II) complexes have been reported in literature which are helpful in distinguishing between 5- or 6-coordinated copper (II) complexes [96,97] while complications are caused by overlapping of expected d-d transitions. The solid state diffuse reflectance spectra of complexes 2–4 showed significantly different spectral band position from that of complex 5 indicating the presence of different chromophores i.e. CuN_4O_2 in complexes 2–4 and CuN_2O_4 in complex 5. In order to understand the stability of complexes 1–3 (coordination geometry) in solution state, UV–vis spectra for all complexes 1–5 were recorded using different solvents ((2:1) mixtures of methanol-water and DMSO- H_2O) (Fig. S3). Complexes 1–5 exhibited broad absorption bands due to d-d transitions at 752 nm ($\epsilon = 120 \text{ M}^{-1} \text{ cm}^{-1}$), 575 nm ($\epsilon = 58 \text{ M}^{-1} \text{ cm}^{-1}$), 560 nm ($\epsilon = 162 \text{ M}^{-1} \text{ cm}^{-1}$), 563 nm ($\epsilon = 188 \text{ M}^{-1} \text{ cm}^{-1}$), 662 nm ($\epsilon = 108 \text{ M}^{-1} \text{ cm}^{-1}$), respectively, indicating that complexes 2–4 have almost similar chromophore while complexes 1 and 5 have different chromophore. However, similar UV–vis spectra of complexes 1–5 in different solvents (methanol:water and DMSO:water) indicated that the chromophoric group remained intact in different solvents (no solvatochromic effect). Furthermore, nearly similar UV–vis spectra in solution state and solid state diffuse reflectance spectra indicated that all complexes retain their structure in solu-

Table 2
Selected bond distances (Å) and angles (°) for complexes **2**, **3** and **5**.

2		3		5	
Bond	Distance (Å)	Bond	Distance (Å)	Bond	Distance (Å)
Cu1—N1	2.006 (3)	Cu1—O1	1.948 (2)	Cu1—N1	2.047 (2)
Cu1—N2	2.013 (2)	Cu1—N1	2.026 (2)	Cu1...O2	2.627 (2)
Cu1—O1W	2.530 (3)	Cu1...O2	2.499 (2)		
2		3		5	
Bonds	Angle (°)	Bonds	Angle (°)	Bonds	Angle (°)
N1—Cu1—N2	84.5 (1)	O1—Cu1—N1	92.8 (1)	N1—Cu1—C4	93.58 (9)
O1W—Cu1—N1	97.1 (1)	N1—Cu1—C4	91.18 (9)	O1—Cu1—O1 ⁱ	92.86 (8)
O1W—Cu1—N2	91.3 (1)	O1—Cu1—O1 ⁱ	87.3 (1)	N1—Cu1—N1 ⁱ	86.8 (1)
N1—Cu1—N2 ⁱ	95.5 (1)	N1—Cu1—N1 ⁱ	87.1 (1)		
O1W—Cu1—N1 ⁱ	82.9 (1)		88.8 (1)		
O1W—Cu1—N2 ⁱ	88.7 (1)		92.6 (1)		
Symmetry code:	(i) 2 − x, 1 − y, 1 − z		(i) 1 − x, 1 − y, −z		(i) −x, y, 1/2 − z

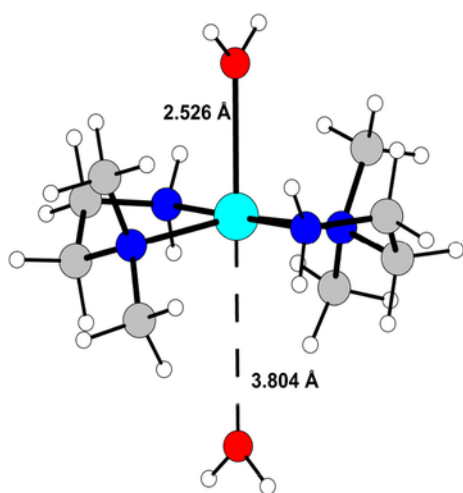


Fig. 4. Optimized geometry of the $[\text{Cu}(\text{unsym-dmen})_2(\text{H}_2\text{O})_2]^{2+}$ cation in complex **4**.

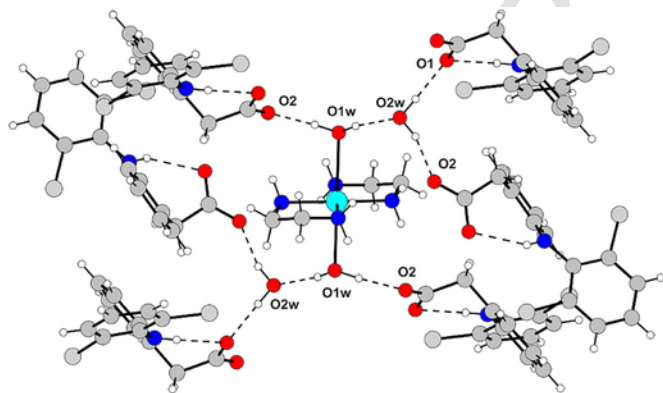


Fig. 5. O—H...O hydrogen bonding network in **2**.

tion as well as in solid state. The solution UV–vis and solid state diffuse reflectance spectra for complexes **2–5** are given in Figs. S3 and S4.

The molar conductivity measurements of the complexes were carried in a 1 mM DMSO solution of the complexes. The obtained Λ_M values revealed the non-electrolytic nature of complexes **1** and **5** ($\Lambda_M = 5\text{--}7 \text{ S cm}^2 \text{ mol}^{-1}$). For complexes **2–4**, the Λ_M values were

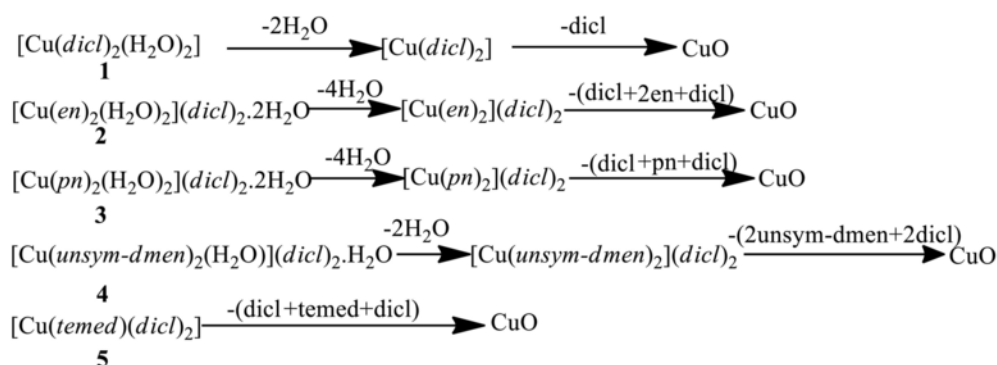
found in the range $30\text{--}40 \text{ S cm}^2 \text{ mol}^{-1}$ which revealed that the complexes partially dissociate in solution in order to provide a partial 1:1 electrolyte nature; nevertheless, we may suggest that complexes **2–4** keep their structures in solution, since an 1:2 electrolyte would be expected in case of full dissociation which could result from a cleavage of the hydrogen bond interactions between the dicationic complex moiety $[\text{Cu}(\text{N,N'}\text{-donor})_2]^{2+}$ and the two anions of diclofenac.

3.4. Thermogravimetric analysis

Thermogravimetric curves for complexes **1–5** (Figs. S5–S9) were recorded under nitrogen atmosphere in order to study the thermal stability of newly synthesized complexes. TGA profiles for complexes **1–4** clearly revealed that all complexes exhibit loss of water molecules in the first transition in the temperature range from 70 to 150 °C. For complex **5**, there is no weight loss observed in this temperature range indicating the absence of water molecule. The second weight loss for complexes **1–5** might be assigned to loss of one weakly coordinated diclofenac molecule in the temperature range 150–270 °C. The weight losses in the temperature range 270–500 °C might be due to loss of nitrogen-donor ligand attached to metal center and another diclofenac molecule. After 500 °C, no significant weight loss have been observed in all cases and appearance of stable curves indicated formation of stable cupric oxide residue. The steps of the thermal decomposition (% weight loss) of all complexes **1–5** are given in Table S3 and Scheme 2.

3.5. Interaction of the complexes with BSA

Albumin is the most common protein in blood plasma having among others the role to transport drugs, metal ions and/or complexes through the blood stream towards cells and tissues. BSA (the most commonly used homologue for human serum albumin) solution (3 μM) exhibits a strong fluorescence emission band at 342 nm, when it is excited at 295 nm [73], which is attributed to the tryptophans found at positions 134 and 212 [75]. The quantitative studies of the BSA fluorescence emission spectra were performed after their correction by subtracting the spectra of the compounds. The addition of compounds **1–5** into the BSA solution resulted in a moderate-to-high quenching (between 55 and 77% of the initial fluorescence intensity) of BSA fluorescence at $\lambda = 342 \text{ nm}$ (Fig. 6). The observed decrease of fluorescence intensity may be mainly attrib-



Scheme 2. TGA profiles indicating loss of different moieties with increase in temperature for complexes 1–5.

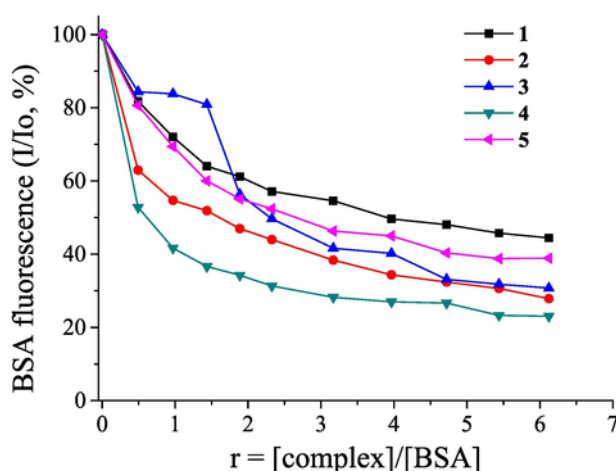


Fig. 6. Plot of % relative BSA (3 μM , in buffer solution of 150 mM NaCl and 15 mM trisodium citrate at pH 7.0) fluorescence emission intensity at $\lambda_{\text{em}} = 342 \text{ nm}$ (I/I_0 , %) versus r ($r = [\text{complex}]/[\text{BSA}]$) for complexes 1–5 (44.5% of the initial fluorescence intensity for 1, 27.9% for 2, 30.8% for 3, 23.1% for 4 and 38.9% for 5).

uted to possible changes in protein secondary structure leading to changes in tryptophan environment of BSA, indicating the binding of each complex to the serum albumin [75].

The Stern-Volmer (K_{sv}) and the quenching (k_q) constant values for complexes 1–5 were calculated by the Stern-Volmer quenching equation (eqs. S2 and S3) and the corresponding Stern-Volmer plots (Fig. S10) and are presented in Table 3. These values are indicative of good quenching ability with the complexes having higher constants than free *Nadicl* with complex 4 presenting the highest k_q value ($K = 3.29(\pm 0.23) \times 10^{13} \text{ M}^{-1} \text{ s}^{-1}$). Furthermore, the derived k_q constants are much higher than the value of

Table 3
The BSA constants (k_q , K) for *Nadicl* and its complexes 1–5.

Compound	k_q ($\text{M}^{-1} \text{ s}^{-1}$)	K (M^{-1})
<i>Nadicl</i> [42]	$8.11(\pm 0.34) \times 10^{12}$	3.55×10^5
$[\text{Cu}(\text{dicl})_2(\text{H}_2\text{O})_2]$, 1	$1.06(\pm 0.08) \times 10^{13}$	$2.49(\pm 0.08) \times 10^5$
$[\text{Cu}(\text{en})_2(\text{H}_2\text{O})_2](\text{dicl})_2$, 2	$1.25(\pm 0.07) \times 10^{13}$	$3.04(\pm 0.13) \times 10^5$
$[\text{Cu}(\text{pn})_2(\text{H}_2\text{O})_2](\text{dicl})_2$, 3	$1.29(\pm 0.06) \times 10^{13}$	$1.10(\pm 0.08) \times 10^5$
$[\text{Cu}(\text{unsym-dmen})_2(\text{H}_2\text{O})_2](\text{dicl})_2$, 4	$3.29(\pm 0.23) \times 10^{13}$	$9.98(\pm 0.29) \times 10^5$
$[\text{Cu}(\text{temed})](\text{dicl})_2$, 5	$1.22(\pm 0.08) \times 10^{13}$	$2.23(\pm 0.09) \times 10^5$

$2.0 \times 10^{10} \text{ M}^{-1} \text{ s}^{-1}$ reported for diverse quenchers for biopolymer fluorescence and may show the existence of static quenching mechanism [73], verifying the interaction of the complexes with BSA.

The SA-binding constants K (Table 4) were calculated by the Scatchard equation (eq. S4) and the corresponding Scatchard plots (Fig. S11). The K constants are relatively high with complex 4 exhibiting the highest K value ($K = 9.98(\pm 0.29) \times 10^5 \text{ M}^{-1}$). In total, the binding constants of the complexes ($K = 1.10 \times 10^5$ – $9.98 \times 10^5 \text{ M}^{-1}$) are high enough to verify the binding of the complexes to BSA in order to get transferred. They are also significantly lower than the value of 10^{15} M^{-1} which is the association constant of the protein avidin with diverse compounds and is among the strongest noncovalent bindings; therefore, the binding of the complexes to BSA may be considered reversible and may reveal their ability to be released upon arrival at their biological targets [98].

3.6. Interaction of the complexes with CT DNA

The interaction mode of metal complexes with double-stranded DNA is mainly dependent on the structure of the complexes and the nature of their ligands. In case of labile ligands, covalent DNA-binding may occur while the stability of the complexes may results to non-covalent DNA-interaction [10–12]. In addition, the field of interaction of metal-NSAID compounds with double-stranded DNA has recently gained increasing research interest, since it may be correlated with potential anticancer, antioxidant and/or anti-inflammatory activities. Within this context, the DNA-binding of complexes 1–5 has been studied *in vitro* by UV-vis spectroscopy, viscosity measurements and cyclic voltammetry and *via* their ability to displace the typical DNA-intercalator EB.

Table 4
Spectral features of the interaction of *Nadicl* and its complexes 1–5 with CT DNA. UV-band (λ in nm) (percentage of the hyper-/hypo-chromism ($\Delta A/A_0$, %), blue-/red-shift of the λ_{max} ($\Delta \lambda$, nm)) and DNA-binding constants (K_b).

Compound	λ (nm) ($\Delta A/A_0$ (%), $\Delta \lambda$ (nm))	K_b (M^{-1})
<i>Nadicl</i> [42]	295 (–7.5, –5)	$3.16(\pm 0.14) \times 10^4$
$[\text{Cu}(\text{dicl})_2(\text{H}_2\text{O})_2]$, 1	275 (+13, 0)	$2.25(\pm 0.15) \times 10^4$
$[\text{Cu}(\text{en})_2(\text{H}_2\text{O})_2](\text{dicl})_2$, 2	270 (–2.5, 0)	$5.85(\pm 0.35) \times 10^5$
$[\text{Cu}(\text{pn})_2(\text{H}_2\text{O})_2](\text{dicl})_2$, 3	285 (–4, 0)	$4.88(\pm 0.08) \times 10^6$
$[\text{Cu}(\text{unsym-dmen})_2(\text{H}_2\text{O})_2](\text{dicl})_2$, 4	274 (–5, 0)	$2.54(\pm 0.06) \times 10^6$
$[\text{Cu}(\text{temed})](\text{dicl})_2$, 5	277 (+5, 0)	$2.73(\pm 0.22) \times 10^5$

3.6.1. Study of the DNA-interaction by UV-vis spectroscopy

UV-vis spectroscopy was initially used to study the DNA-binding mode and to calculate its strength magnitude. Any changes observed in the DNA-band or the intraligand transition bands of the complexes may reveal the existence of interaction and its possible mode. The UV-vis spectra of CT DNA solution ($1.2\text{--}1.4 \times 10^{-4}\text{M}$) were recorded in the presence of increasing amounts of complexes 1–5 and exhibited similar changes (representatively shown for in the presence of complex 4 in Fig. 7(A)). A slight hyperchromism of the DNA UV-band at 258 nm was observed indicating the interaction of the complexes with CT DNA [99].

Additionally, the UV-vis spectra of complexes 1–5 ($10\text{--}20\text{ }\mu\text{M}$) were recorded in the presence of increasing amounts of CT DNA. The step-wise additional of CT DNA in the solution of the complexes resulted in a slight hypochromism up to 5% (for complexes 2–4, Fig. 7(B)) or hyperchromism up to 13% (for complexes 1 and 5, Fig. 7(C)) of the intraligand band of the complexes located in the region 270–285 nm (Table 4), while the position of the band did not show any appreciable shift. The findings from the UV-vis spectroscopic titrations may reveal the binding of complexes to CT DNA, although no final conclusion regarding the mode of this binding may be suggested; thus, additional studies involving DNA-viscosity measurements and cyclic voltammetry were carried out in order to conclude the DNA-binding fashion [100,101].

The values of the binding constant K_b of complexes 1–5 with CT DNA were calculated by the Wolfe-Shimer equation (eq. S5) [76] and the respective plots $[\text{DNA}]/(\epsilon_A - \epsilon_f)$ versus DNA (Fig. S12). The K_b values of complexes (Table 4) are significantly higher than that of free *Nadicl*. A quite strong binding of the compounds to DNA is suggested with complex 3 bearing the highest K_b value ($K_b = 4.88(\pm 0.08) \times 10^6\text{ M}^{-1}$) among the present complexes. The K_b values are of the same magnitude to that of the classical intercalator EB ($K_b = 1.23(\pm 0.07) \times 10^5\text{ M}^{-1}$) as calculated by Dimitrakopoulou et al. [102]. The K_b constants are in the range reported for other metal complexes with NSAIDs as ligands [59–66].

3.6.2. Study of the DNA-interaction by DNA-viscosity changes

Viscosity measurements may be an essential tool in order to clarify the mode of interaction of a compound with DNA, because the viscosity of DNA solution is sensitive and related to DNA-length changes [103]. The viscosity of CT DNA solution (0.1 mM) was measured upon addition of increasing amounts of complexes 1–5. The presence of increasing amounts of the complexes led to an increase of the relative DNA-viscosity (Fig. 8). As it is known, in the case of classic intercalation (insertion of the complex in between the DNA base pairs), an increase of the separation distance of DNA-base pairs at intercalation sites takes place in order to host the bound compound; since the relative DNA-viscosity is proportional to the relative DNA-length, the increase of the length of the DNA helix induces an increase of DNA-viscosity, having a magnitude proportional to the strength of the interaction. Therefore, from the observed increase of DNA-viscosity we may conclude the existence of an intercalative interaction between the complexes and CT DNA [103] which seems to be much more pronounced in the case of complexes 1 and 5. These conclusions may reveal the DNA-binding fashion of complexes 1–5.

3.6.3. Study of the DNA-interaction by cyclic voltammetry

The interaction of the metal complexes with DNA was also studied by cyclic voltammetry. The electrochemical techniques are often a useful complement to spectroscopic methods and may offer information concerning the mode and the strength of interaction

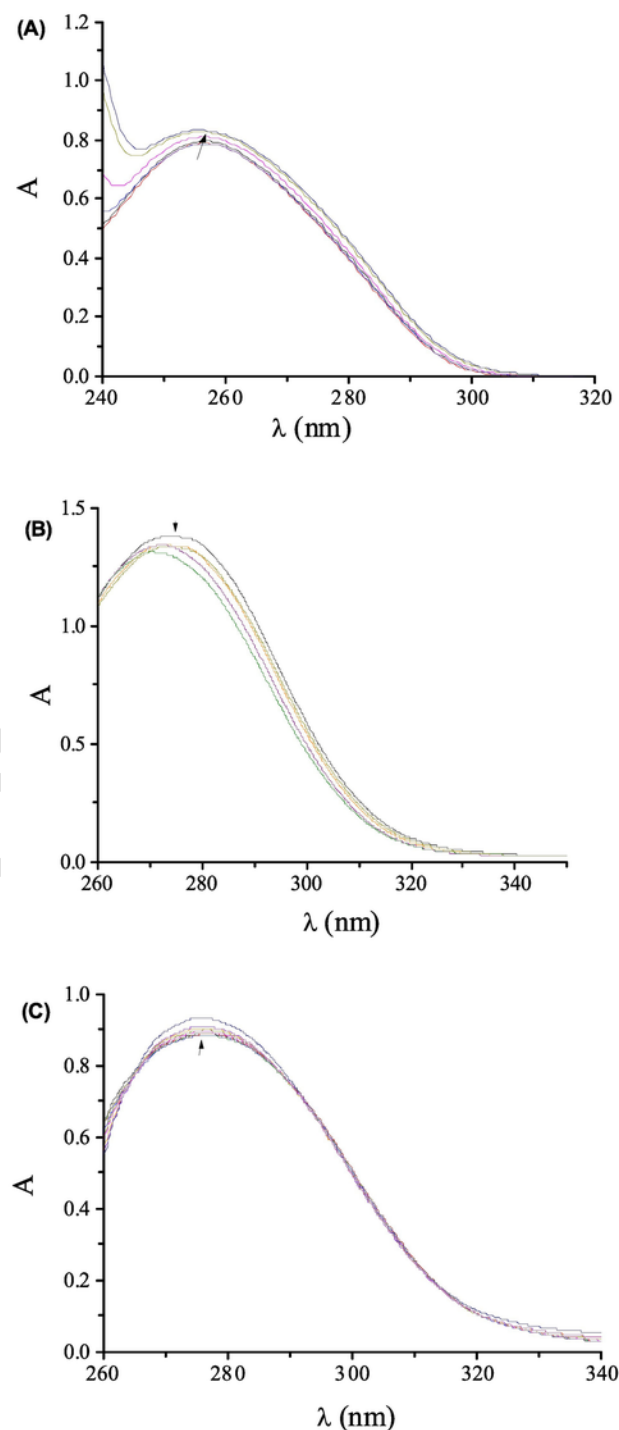


Fig. 7. (A) UV-vis spectra of CT DNA ($[\text{DNA}] = 0.12\text{ mM}$) in buffer solution (150 mM NaCl and 15 mM trisodium citrate at pH 7.0) in the absence or presence of complex 4. The arrows show the changes upon increasing amount of the complex. (B–C) UV-vis spectra of DMSO solution of (B) complex 4 ($[4] = 2 \times 10^{-5}\text{ M}$) and (C) complex 5 ($[5] = 10^{-5}\text{ M}$) in the absence or presence of increasing amounts of CT DNA. The arrows show the changes upon increasing amount of CT DNA.

with both the reduced and oxidized form of the metal. In general, when the metal complex binds to DNA *via* intercalation, the electrochemical potential presents a positive shift, while, in the case of electrostatic binding, the potential will shift to negative values. Furthermore, a positive shift of E_{p1} and a simultaneous negative

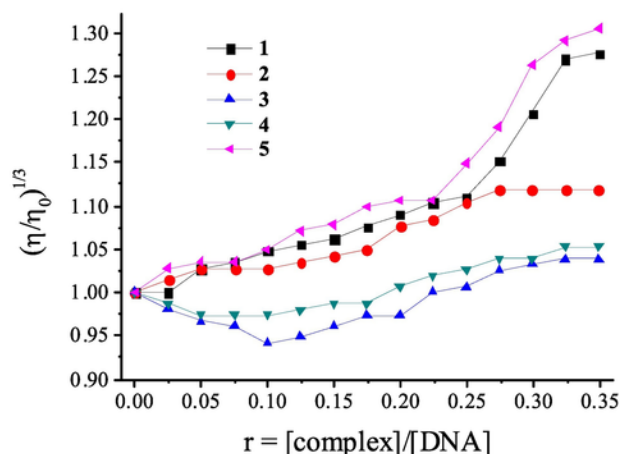


Fig. 8. Relative viscosity of CT DNA $(\eta/\eta_0)^{1/3}$ in buffer solution (150 mM NaCl and 15 mM trisodium citrate at pH 7.0) versus r ($r = [\text{complex}]/[\text{DNA}]$) for complexes 1–5.

shift of E_{p2} may imply that the molecule may interact with DNA by both ways [57].

The cyclic voltammogram of complexes 1–5 in a 1:2 DMSO:buffer solution (0.33 mM) was recorded upon addition of CT DNA solution (Fig. S13) and the shifts of the cathodic (E_{pc}) and anodic (E_{pa}) potentials of the complexes are given in Table 5. No new redox peaks appeared after the addition of CT DNA. The electrochemical behavior of all complexes was similar upon addition of DNA and both the cathodic and the anodic potentials exhibited a positive shift ($\Delta E_{pc/a} = (+3) - (+48)$ mV) showing the existence of intercalation between the complexes and CT DNA bases [77]. Such conclusion is in good agreement with the viscosity experiments and further clarifies the UV–vis spectroscopic findings.

In addition, the corresponding equilibrium constants for the redox process of the complexes were evaluated by determining the ratio of the DNA-binding constants for the reduced (K_r) and oxidized forms (K_{ox}) of the metal ions (K_r/K_{ox}) according to eq. S6 [77]. The ratio K_r/K_{ox} of the redox process for the complexes is found in the range 1.27–1.78 and indicates that the binding of DNA is stronger for the reduced than the oxidized form of the complexes [104].

3.6.4. Competitive studies with ethidium bromide

Ethidium bromide is a typical indicator of intercalation [105]. EB intercalates through its planar phenanthridine ring in-between adjacent DNA bases forming an EB-DNA conjugate which presents an intense fluorescence emission band at 592 nm. Upon addition of the complexes into the EB-DNA solution, the changes observed in the fluorescence emission spectra of the EB-DNA conjugate may be used to evaluate the ability of the complexes to displace EB from

the EB-DNA conjugate and subsequently to intercalate to DNA equally or even more strongly than EB.

The fluorescence emission spectra of EB-DNA in the absence and presence of complexes 1–5 were recorded for $[\text{EB}] = 20 \mu\text{M}$, $[\text{DNA}] = 26 \mu\text{M}$ for increasing amounts of each complex. The addition of complexes 1–5 at diverse r values (representatively shown for complex 3 in Fig. 9(A)) resulted in a remarkable decrease of intensity of the characteristic EB-DNA emission band at 592 nm. The fluorescence quenching is up to 83.5% of the initial EB-DNA fluorescence intensity (Fig. 9(B), Table 6) indicating the competition of the complexes with EB in their binding to DNA; complexes 1–5 may displace EB from the DNA-EB conjugate, interacting with CT DNA by the intercalative mode [78].

The linear Stern-Volmer equation (eq. S4) and the corresponding Stern-Volmer plots of EB-DNA ($R = 0.99$, Fig. S14) proved that the EB-DNA fluorescence emission quenching is a result of the displacement of EB from EB-DNA by each complex 1–5. The calculated values of K_{sv} (Table 6) show that complexes 1–5 bind to DNA rather tightly and complex 5 bears the highest K_{sv} value ($K_{sv} = 4.00(\pm 0.13) \times 10^6 \text{ M}^{-1}$) among the present compounds. Since the fluorescence lifetime of the EB-DNA system is $\tau_0 = 23 \text{ ns}$ [79], the EB-DNA quenching constants for the compounds were calculated according to eq. S3. The calculated k_q constants (Table 7) are much higher than the value of $10^{10} \text{ M}^{-1} \text{ s}^{-1}$; such high k_q values may reveal that the quenching of the EB-DNA fluorescence induced by the complexes takes place via a static mechanism [73] and leads to the formation of a new conjugate, i.e. between each complex and DNA.

3.7. Comparison of the binding constants

The present copper(II) complexes 1–5 may be compared with the so far reported metal(II)-diclofenac complexes, i.e. Cu(II), Ni(II) and Mn(II) complexes with diverse heterocyclic nitrogen-donor ligands pyridine (py), 1,10-phenanthroline (phen), 2,2'-dipyridylketone oxime (Hpko), 2,2'-bipyridine (bipy) and 2,2'-bipyridylamine (bipyam) [42,46,50], in regard their BSA-binding, DNA-binding, and EB-displacing ability constants (Table 7).

In regard to the affinity of the compounds to BSA, a comparison with the reported metal-diclofenac complexes may reveal that the BSA-binding constants of complexes 1–5 are of the same magnitude with those of the Ni(II)- and Mn(II)-diclofenac complexes, especially the cationic complexes $[\text{Ni}(\text{dicl})(\text{Hdicl})(\text{Hpko})_2](\text{dicl})$ [50] and $[\text{Mn}(\text{dicl})(\text{bipy})(\text{H}_2\text{O})_2](\text{dicl})$ [46], and higher than those of the neutral copper(II) complexes (Table 7).

A comparison of the DNA-binding constants with the reported metal complexes of diclofenac [42,46,50] may reveal that the present complexes 1–5, and especially the cationic complexes, exhibit among the highest K_b constants, while a concrete conclusion regarding their EB-displacing ability cannot arise since all K_{sv} constants have rather similar values (Table 7).

Table 5

Cathodic and anodic potentials (in mV) for the redox couple Cu(II)/Cu(I) of complexes 1–5 in 1/2 DMSO:buffer solution in the absence or presence of CT DNA.

Complex	$E_{pc(a)}$ ^a	$E_{pc(b)}$ ^b	ΔE_{pc} ^c	$E_{pa(a)}$ ^a	$E_{pa(b)}$ ^b	ΔE_{pa} ^c	K_r/K_{ox}
$[\text{Cu}(\text{dicl})_2(\text{H}_2\text{O})_2]$, 1	−777	−725	+52	−428	−425	+3	1.59
$[\text{Cu}(\text{en})_2(\text{H}_2\text{O})_2](\text{dicl})_2$, 2	−801	−795	+6	−428	−406	+22	1.27
$[\text{Cu}(\text{pn})_2(\text{H}_2\text{O})_2](\text{dicl})_2$, 3	−709	−689	+20	−433	−385	+48	1.78
$[\text{Cu}(\text{unsym-dmen})_2(\text{H}_2\text{O})_2](\text{dicl})_2$, 4	−725	−715	+10	−427	−399	+28	1.38
$[\text{Cu}(\text{temed})(\text{dicl})_2]$, 5	−741	−721	+20	−489	−445	+44	1.72

^a $E_{pc/a}$ in DMSO:buffer in the absence of CT DNA ($E_{pc/a(a)}$).

^b $E_{pc/a}$ in DMSO:buffer in the presence of CT DNA ($E_{pc/a(b)}$).

^c $\Delta E_{pc/a} = E_{pc/a(b)} - E_{pc/a(a)}$.

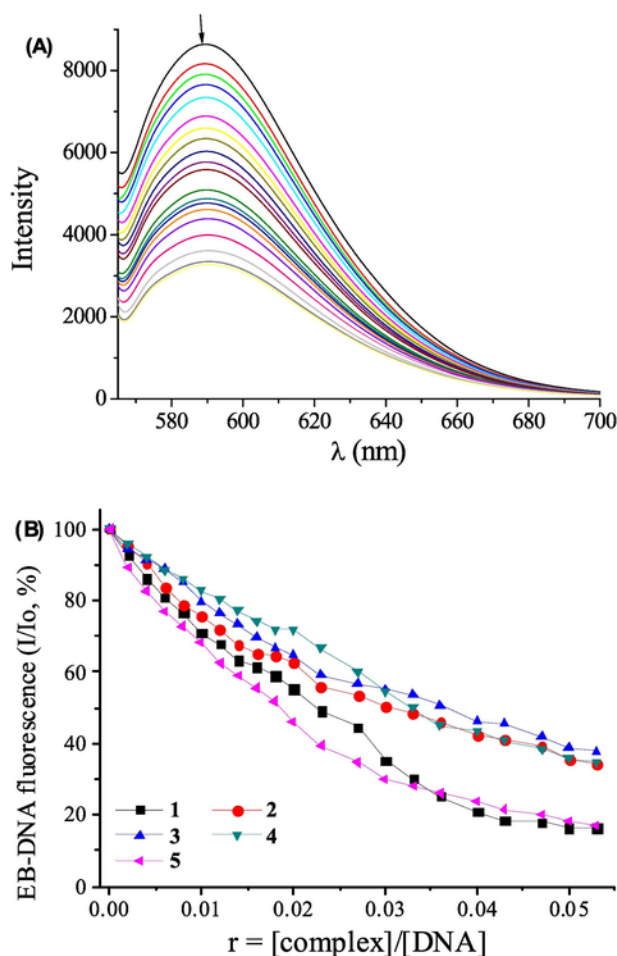


Fig. 9. (A) Fluorescence emission spectra ($\lambda_{\text{exc}} = 540 \text{ nm}$) for EB-DNA ($[\text{EB}] = 20 \mu\text{M}$, $[\text{DNA}] = 26 \mu\text{M}$) in buffer solution in the absence and presence of increasing amounts of complex 3 (up to the value of $r = 0.055$). The arrow shows the changes of intensity upon increasing amounts of complex 3. (B) Plot of relative EB-DNA fluorescence intensity (I/I_0 , %) at $\lambda_{\text{em}} = 592 \text{ nm}$ versus r ($r = [\text{complex}]/[\text{DNA}]$) in buffer solution (150 mM NaCl and 15 mM trisodium citrate at pH 7.0) in the presence of complexes 1–5 (quenching up to 16.5% of the initial EB-DNA fluorescence for 1, 34.2% for 2, 37.9% for 3, 34.8% for 4 and 17.2% for 5).

Among the copper-diclofenac compounds, it seems that the presence of diclofenac in the anionic form as a counter anion as in complexes 2–4 results in much higher DNA- and BSA-binding constants than the compounds where diclofenac is coordinated to copper. A concrete conclusion regarding the role of the metal ion (Cu(II), Mn(II) or Ni(II)) in the biological activity cannot be definitely arisen, because there are not reported Mn(II) and Ni(II) diclofenac compounds with aliphatic nitrogen-donors ligands.

Table 6

Fluorescence features of the EB-displacement studies of *Nadicl* and its complexes 1–5. Percentage of EB-DNA fluorescence quenching ($\Delta I/I_0$, %), Stern-Volmer (K_{SV}) and fluorescence quenching constants (k_q).

Compound	$\Delta I/I_0$ (%)	K_{SV} (M^{-1})	k_q ($\text{M}^{-1} \text{s}^{-1}$)
<i>Nadicl</i> [42]	65.0	$2.47(\pm 0.06) \times 10^5$	$1.07(\pm 0.03) \times 10^{13}$
$[\text{Cu}(\text{dicl})_2(\text{H}_2\text{O})_2]$, 1	83.5	$1.96(\pm 0.07) \times 10^6$	$8.50(\pm 0.30) \times 10^{13}$
$[\text{Cu}(\text{en})_2(\text{H}_2\text{O})_2](\text{dicl})_2$, 2	65.8	$7.43(\pm 0.12) \times 10^5$	$3.23(\pm 0.05) \times 10^{13}$
$[\text{Cu}(\text{pn})_2(\text{H}_2\text{O})_2](\text{dicl})_2$, 3	62.1	$1.26(\pm 0.03) \times 10^5$	$5.50(\pm 0.11) \times 10^{12}$
$[\text{Cu}(\text{unsym-dmen})_2(\text{H}_2\text{O})](\text{dicl})_2$, 4	65.2	$3.97(\pm 0.11) \times 10^5$	$1.73(\pm 0.05) \times 10^{13}$
$[\text{Cu}(\text{temed})(\text{dicl})_2]$, 5	82.8	$4.00(\pm 0.13) \times 10^6$	$1.74(\pm 0.06) \times 10^{14}$

4. Conclusions

Four new copper(II)-diclofenac complexes have been synthesized in the presence of different nitrogen-donor ligands using methanol-water (4:1 v/v) as solvent in quantitative yields at room temperature along with previously reported $[\text{Cu}(\text{dicl})_2(\text{H}_2\text{O})_2]$, 1. The newly synthesized copper(II) complexes were characterized by spectroscopic methods (UV-vis, FT-IR) and thermogravimetric analyses. The crystal structures of complexes 2, 3 and 5 have been unambiguously determined with single-crystal X-ray crystallography indicating the ionic structure of complexes 2 and 3 and the neutral structure of complex 5. DFT calculations provided insight into the possible existence of square pyramidal or octahedral geometry of complex 4 which is in good agreement with spectroscopic data and the research within the Cambridge Crystallographic Database.

Complexes 1–5 present significant affinity for bovine serum albumin, as monitored by fluorescence emission spectroscopy. The complexes bind reversibly to the BSA for their potential transportation towards their biological targets. Complexes 1–5 may bind to CT DNA probably *via* intercalation in-between DNA-bases, as revealed by the techniques used, and bind to CT DNA much tighter than the free NSAID sodium diclofenac does. Complex $[\text{Cu}(\text{pn})_2(\text{H}_2\text{O})_2](\text{dicl})_2$, 3, exhibits the highest DNA-binding constant ($K_b = 4.88(\pm 0.08) \times 10^6 \text{ M}^{-1}$) among the studied complexes 1–5. The present *in vitro* behavior of complexes 1–5 concerning their binding to BSA and CT DNA may be considered promising for more biological studies and their potential application as metal-lopharmaceutical agents.

Abbreviations

<i>bipy</i>	2,2'-bipyridine
<i>bipyam</i>	2,2'-bipyridylamine
BSA	bovine serum albumin
CT	calf-thymus
<i>dicl</i>	deprotonated diclofenac
EB	ethidium bromide
<i>en</i>	Ethylenediamine
<i>Hdicl</i>	Diclofenac
<i>Hpko</i>	2,2'-dipyridylketone oxime
K	BSA-binding
K_b	DNA-binding constant
k_q	quenching constant
K_{SV}	Stern-Volmer constant
<i>Nadicl</i>	sodium diclofenac
NSAID	non-steroidal anti-inflammatory drug
<i>phen</i>	1,10-phenanthroline
<i>pn</i>	propan-1,3-diamine
<i>py</i>	Pyridine
<i>r</i>	$[\text{complex}]/[\text{DNA}]$ mixing ratio

Table 7

The BSA-binding (K_{BSA} , in M^{-1}), DNA-binding (K_b , in M^{-1}) and EB-DNA Stern-Volmer (K_{SV} , in M^{-1}) constants of complexes 1–5 and reported metal complexes of diclofenac.

Compound	K_{BSA} (M^{-1})	K_b (M^{-1})	K_{SV} (M^{-1})
Nadcl [42]	3.55×10^5	$3.16(\pm 0.14) \times 10^4$	$2.47(\pm 0.06) \times 10^5$
[Cu(dicl) ₂ (H ₂ O) ₂], 1	$2.49(\pm 0.08) \times 10^5$	$2.25(\pm 0.15) \times 10^4$	$1.96(\pm 0.07) \times 10^6$
[Cu(en) ₂ (H ₂ O) ₂](dicl) ₂ , 2	$3.04(\pm 0.13) \times 10^5$	$5.85(\pm 0.35) \times 10^5$	$7.43(\pm 0.12) \times 10^5$
[Cu(pn) ₂ (H ₂ O) ₂](dicl) ₂ , 3	$1.10(\pm 0.08) \times 10^5$	$4.88(\pm 0.08) \times 10^6$	$1.26(\pm 0.03) \times 10^5$
[Cu(unsym-dmen) ₂ (H ₂ O)](dicl) ₂ , 4	$9.98(\pm 0.29) \times 10^5$	$2.54(\pm 0.06) \times 10^6$	$3.97(\pm 0.11) \times 10^5$
[Cu(temed)(dicl) ₂], 5	$2.23(\pm 0.09) \times 10^5$	$2.73(\pm 0.22) \times 10^5$	$4.00(\pm 0.13) \times 10^6$
[Cu(dicl) ₂ (phen)] [42]	1.62×10^5	$1.81(\pm 0.13) \times 10^4$	$4.82(\pm 0.15) \times 10^5$
[Cu(dicl) ₂ (py) ₂] [42]	5.63×10^4	$4.35(\pm 0.25) \times 10^3$	$1.35 \pm (0.22) \times 10^4$
[Cu ₂ (dicl) ₄ (H ₂ O) ₂] [42]	1.72×10^5	$1.74(\pm 0.45) \times 10^4$	$6.98(\pm 0.34) \times 10^5$
[Ni(dicl)(Hdicl)(Hpko) ₂](dicl) [50]	$2.21(\pm 0.23) \times 10^5$	$3.63(\pm 0.12) \times 10^5$	$1.40(\pm 0.03) \times 10^5$
[Ni(dicl) ₂ (bipy)] [50]	$1.31(\pm 0.11) \times 10^6$	$2.21(\pm 0.08) \times 10^5$	$9.43(\pm 0.20) \times 10^5$
[Ni(dicl) ₂ (phen)] [50]	$1.72(\pm 0.13) \times 10^5$	$3.67(\pm 0.17) \times 10^4$	$1.07(\pm 0.04) \times 10^6$
[Mn ₃ (dicl) ₆ (phen) ₂ (MeOH)] [46]	$1.15(\pm 0.06) \times 10^6$	$3.60(\pm 0.35) \times 10^4$	$6.63(\pm 0.34) \times 10^5$
[Mn(dicl) ₂ (bipyam)] [46]	$3.14(\pm 0.16) \times 10^6$	$3.59(\pm 0.27) \times 10^4$	$7.80(\pm 0.42) \times 10^5$
[Mn(dicl)(bipy)(H ₂ O) ₂](dicl) [46]	$3.18(\pm 0.19) \times 10^5$	$1.24(\pm 0.08) \times 10^5$	$4.98(\pm 0.30) \times 10^6$
[Mn(dicl) ₂ (py) ₂ (H ₂ O) ₂] [46]	$2.30(\pm 0.13) \times 10^5$	$4.56(\pm 0.26) \times 10^5$	$1.61(\pm 0.28) \times 10^6$

temed *N,N,N',N'*-tetramethylethylenediamine

unsym-dmen unsymmetrical dimethylethylene-diamine

 $\Delta\nu(\text{COO}) = \nu_{\text{asym}}(\text{COO}) - \nu_{\text{sym}}(\text{COO})$

Acknowledgements

The authors RPS and SK acknowledge the financial support from UGC, New Delhi (India) as a UGC Emeritus and BSR Meritorious Fellowship, respectively. PV thanks the DST PURSE program of Panjab University, Chandigarh. This research was also financed (via a scholarship to SP) by the General Secretariat for Research and Technology (GSRT) and Hellenic Foundation for Research and Innovation (HFRI), Greek Ministry of Education, Research and Religion.

Appendix A. Supplementary material

Crystallographic data for the structural analysis of the three new compounds have been deposited at the Cambridge Crystallographic Data Center, 12 Union Road, Cambridge, CB2 1EZ, UK, and are available free of charge from the Director on request quoting the deposition number CCDC 1583609–1583611 for complexes 2, 3 and 5, respectively. Supplementary data associated with this article can be found, in the on-line version, at doi:https://doi.org/10.1016/j.jinorgbio.2018.07.009.

References

- [1] B. Rosenberg, L.V. Camp, T. Krigas, Nature 205 (1965) 698–699.
- [2] B. Rosenberg, L.V. Camp, J.E. Trosko, V.H. Mansour, Nature 222 (1969) 385–386.
- [3] S. Medici, M. Peana, V.M. Nurchi, J.I. Lachowicz, G. Crisponi, M.A. Zoroddu, Coord. Chem. Rev. 284 (2015) 329–350.
- [4] L. Ronconi, P.J. Sadler, Coord. Chem. Rev. 251 (2007) 1633–1648.
- [5] N. Farrell, in: J.A. McCleverty, T.J. Meyer (Eds.), Comprehensive Coordination Chemistry II, Pergamon, Oxford, 2003, pp. 809–840.
- [6] Z. Guo, P.J. Sadler, Angew. Chem. Int. Ed. 38 (1999) 1512–1531.
- [7] K. Gurova, Future Oncol. 5 (2009) 1685–1704.
- [8] U. Pindur, M. Jansen, T. Lemster, Curr. Med. Chem. 12 (2005) 2805–2847.
- [9] L. Strekowski, B. Wilson, Mutat. Res. 623 (2007) 3–13.
- [10] K.E. Erkkila, D.T. Odom, J.K. Barton, Chem. Rev. 99 (1999) 2777–2795.
- [11] A.C. Komor, J.K. Barton, Chem. Commun. 49 (2013) 3617–3630.
- [12] B.M. Zeglis, V.C. Pierre, J.K. Barton, Chem. Commun. (2007) 4565–4579.
- [13] J.R.J. Sorenson, Biology of Copper Complexes, Humana Press, 1987.
- [14] G. Gisponi, V.M. Nurchi, D. Fanni, C. Gerosé, S. Nimaloto, G. Faa, Coord. Chem. Rev. 254 (2010) 876–889.
- [15] P. Chellan, P.J. Sadler, Phil. Trans. R. Soc. A 373 (2015) 20140182.
- [16] W.X. Tian, S. Yu, M. Ibrahim, A.W. Almonaofy, L. He, Q. Hui, Z. Bo, B. Li, G.L. Xie, J. Microbiol. 50 (2012) 586–593.
- [17] S. Medici, M. Peana, V.M. Nurchi, J.I. Lachowicz, G. Crisponi, M.A. Zoroddu, Coord. Chem. Rev. 284 (2015) 329–350.
- [18] P. Fernandes, I. Sousa, L. Cunha-Silva, M. Ferreira, B. de Castro, E.F. Pereira, M.J. Feio, P. Gameiro, J. Inorg. Biochem. 131 (2014) 21–29.
- [19] B. Chudzik, I.B. Tracz, G. Czernel, M.J. Fiolka, G. Borsuk, M. Gagos, Eur. J. Pharm. Sci. 49 (2013) 850–857.
- [20] M. Gziut, H.J. MacGregor, T.G. Nevell, T. Mason, D. Laight, J.K. Shute, Br. J. Pharmacol. 168 (2013) 1165–1181.
- [21] J. Nagaj, R. Starosta, M. Jezowska-Bojczuk, J. Inorg. Biochem. 142 (2015) 68–74.
- [22] G.J. Brewer, Curr. Opin. Chem. Biol. 7 (2003) 207–212.
- [23] B.M. Paterson, P.S. Donnelly, Chem. Soc. Rev. 40 (2011) 3005–3018.
- [24] J.E. Weder, C.T. Dillon, T.W. Hambley, B.J. Kennedy, P.A. Lay, J.R. Biffin, H.L. Regtop, N.M. Davies, Coord. Chem. Rev. 232 (2002) 95–126.
- [25] C. Santini, M. Pellei, V. Gandini, M. Porchia, F. Tisato, C. Marzano, Chem. Soc. Rev. 114 (2014) 815–862.
- [26] W.C. Zhang, X. Tang, X. Lu, J. Inorg. Biochem. 156 (2016) 105–112.
- [27] K. Alomar, A. Landreau, M. Allain, G. Bouet, G. Larcher, J. Inorg. Biochem. 126 (2013) 76–83.
- [28] R.S. Hoonur, B.R. Patil, D.S. Badiger, R.S. Vadavi, K.B. Gudasi, P.R. Dandawate, M.M. Ghasias, S.B. Padhye, M. Nethaji, Eur. J. Med. Chem. 45 (2010) 2277–2282.
- [29] M.L. Beeton, J.R. Aldrich-Wright, A. Bolhuis, J. Inorg. Biochem. 140 (2014) 167–172.
- [30] C. Tolia, A.N. Papadopoulos, C.P. Raptopoulos, V. Psycharis, C. Garino, L. Salassa, G. Psomas, J. Inorg. Biochem. 123 (2013) 53–65.
- [31] W.J. Wechter, E.D. Murray, D. Kantoci, D.D. Quiggle, D.D. Leipold, K.M. Gibson, J.D. McCracken, Life Sci. 66 (2000) 745–753.
- [32] M.L. Smith, G. Hawcroft, M.A. Hull, Eur. J. Cancer 36 (2000) 664–674.
- [33] A. Inoue, S. Muranaka, H. Fujita, T. Kanno, H. Tamai, K. Utsumi, Free Radic. Biol. Med. 37 (2004) 1290–1299.
- [34] M.J. Gomez-Lechon, X. Ponsoda, E. O'Connor, T. Donato, J.V. Castell, R. Jover, Biochem. Pharmacol. 66 (2003) 2155–2167.
- [35] T. Zhang, T. Otevel, Z.Q. Gao, Z.P. Gao, S.M. Ehrlich, J.Z. Fields, B.M. Boman, Cancer Res. 61 (2001) 8664–8667.
- [36] S. Roy, R. Banerjee, M. Sarkar, J. Inorg. Biochem. 100 (2006) 1320–1331.
- [37] S. Tsiliou, L.-A. Kefala, A.G. Hatzidimitriou, D.P. Kessissoglou, F. Perdih, A.N. Papadopoulos, I. Turel, G. Psomas, J. Inorg. Biochem. 160 (2016) 125–139.
- [38] E.E. Errandonea, I. Oyarzabal, J. Cepeda, E.S. Sebastian, A.R. Dieguez, J.M. Seco, New J. Chem. 41 (2017) 5467–5475.
- [39] S. Sayen, A. Carlier, M. Tarpin, E. Guillon, J. Inorg. Biochem. 120 (2013) 39–43.
- [40] S.B. Etcheverry, D.A. Barrio, A.M. Cortizo, P.A.M. Williams, J. Inorg. Biochem. 88 (2002) 94–100.
- [41] J.E. Weder, T.W. Hambley, B.J. Kennedy, P.A. Lay, G.J. Foran, A.M. Rich, Inorg. Chem. 40 (2001) 1295–1302.

- [42] F. Dimiza, F. Perdih, V. Tangoulis, I. Turel, D.P. Kessissoglou, G. Psomas, J. Inorg. Biochem. 105 (2011) 476–489.
- [43] D. Kovala-Demertzi, A. Theodorou, M.A. Demertzis, C.P. Raptopoulou, A. Terzis, J. Inorg. Biochem. 65 (1997) 151–157.
- [44] A. Tarushi, C.P. Raptopoulou, V. Psycharis, C.K. Kontos, D.P. Kessissoglou, A. Scorilas, V. Tangoulis, G. Psomas, Eur. J. Inorg. Chem. (2016) 219–231.
- [45] M. Zampakou, V. Tangoulis, C.P. Raptopoulou, V. Psycharis, A.N. Papadopoulos, G. Psomas, Eur. J. Inorg. Chem. (2015) 2285–2294.
- [46] M. Zampakou, A.G. Hatzidimitriou, A.N. Papadopoulos, G. Psomas, J. Coord. Chem. 68 (2015) 4355–4372.
- [47] A. Tarushi, A.G. Hatzidimitriou, M. Estrader, D.P. Kessissoglou, V. Tangoulis, G. Psomas, Inorg. Chem. 56 (2017) 7048–7057.
- [48] D. Kovala-Demertzi, D. Mentzafos, A. Terzis, Polyhedron 12 (1993) 1361–1370.
- [49] N. Kourkoulis, M.A. Demertzis, D. Kovala-Demertzi, A. Koutsodimou, A. Moukarika, Spectrochim. Acta A 60 (2004) 2253–2259.
- [50] M. Kyropoulou, C.P. Raptopoulou, V. Psycharis, G. Psomas, Polyhedron 61 (2013) 126–136.
- [51] R.P. Sharma, A. Saini, S. Kumar, P. Venugopalan, V. Ferretti, J. Mol. Struct. 1060 (2014) 256–262.
- [52] S. Kumar, R.P. Sharma, P. Venugopalan, T. Aree, V. Ferretti, J. Mol. Struct. 1092 (2015) 225–231.
- [53] S. Kumar, R.P. Sharma, A. Saini, P. Venugopalan, V. Ferretti, J. Mol. Struct. 1083 (2015) 398–404.
- [54] R.P. Sharma, S. Kumar, P. Venugopalan, V.S. Gondil, S. Chhibber, J. Jezierska, V. Ferretti, Inorg. Chim. Acta 449 (2016) 52–59.
- [55] A. Ozarowski, C.J. Calzado, R.P. Sharma, S. Kumar, J. Jezierska, C. Angeli, F. Spizzo, V. Ferretti, Inorg. Chem. 54 (2015) 11916–11944.
- [56] R.P. Sharma, A. Saini, S. Kumar, J. Kumar, R. Sathishkumar, P. Venugopalan, J. Mol. Struct. 1128 (2017) 135–141.
- [57] R.P. Sharma, S. Kumar, P. Venugopalan, V. Ferretti, A. Tarushi, G. Psomas, M. Witwicki, RSC Adv. 6 (2016) 88546–88556.
- [58] S. Kumar, S. Garg, R.P. Sharma, P. Venugopalan, L. Tenti, V. Ferretti, L. Nivelle, M. Tarpin, E. Guillon, New J. Chem. 41 (2017) 8253–8262.
- [59] G. Psomas, D.P. Kessissoglou, Dalton Trans. 42 (2013) 6252–6276.
- [60] A.A. Tarushi, P. Kastanias, C.P. Raptopoulou, V. Psycharis, D.P. Kessissoglou, A.N. Papadopoulos, G. Psomas, J. Inorg. Biochem. 163 (2016) 332–345.
- [61] A. Tarushi, C. Kakoulidou, C.P. Raptopoulou, V. Psycharis, D.P. Kessissoglou, I. Zoi, A.N. Papadopoulos, G. Psomas, J. Inorg. Biochem. 170 (2017) 85–97.
- [62] A. Tarushi, C.P. Raptopoulou, V. Psycharis, D.P. Kessissoglou, A.N. Papadopoulos, G. Psomas, J. Inorg. Biochem. 140 (2014) 185–198.
- [63] S. Perontsis, A.G. Hatzidimitriou, O.-A. Begou, A.N. Papadopoulos, G. Psomas, J. Inorg. Biochem. 162 (2016) 22–30.
- [64] A. Tarushi, S. Perontsis, A.G. Hatzidimitriou, A.N. Papadopoulos, D.P. Kessissoglou, G. Psomas, J. Inorg. Biochem. 149 (2015) 68–79.
- [65] X. Totta, A.G. Hatzidimitriou, A.N. Papadopoulos, G. Psomas, New J. Chem. 41 (2017) 4478–4492.
- [66] M. Zampakou, N. Rizeq, V. Tangoulis, A.N. Papadopoulos, F. Perdih, I. Turel, G. Psomas, Inorg. Chem. 53 (2014) 2040–2052.
- [67] F. Dimiza, S. Fountoulaki, A.N. Papadopoulos, C.A. Kontogiorgis, V. Tangoulis, C.P. Raptopoulou, V. Psycharis, A. Terzis, D.P. Kessissoglou, G. Psomas, Dalton Trans. 40 (2011) 8555–8568.
- [68] S. Fountoulaki, F. Perdih, I. Turel, D.P. Kessissoglou, G. Psomas, J. Inorg. Biochem. 105 (2011) 1645–1655.
- [69] B.P. Esposito, R. Najjar, Coord. Chem. Rev. 232 (2002) 137–149.
- [70] J. Marmur, J. Mol. Biol. 3 (1961) 208–211.
- [71] M.F. Reichmann, S.A. Rice, C.A. Thomas, P. Doty, J. Am. Chem. Soc. 76 (1954) 3047–3053.
- [72] M.A. Malati, Experimental Inorganic/Physical Chemistry, Woodhead Publishing Limited, 1999.
- [73] J.R. Lakowicz, Principles of Fluorescence Spectroscopy, third ed., Plenum Press, New York, 2006.
- [74] L. Stella, A.L. Capodilupo, M. Bietti, Chem. Commun. (2008) 4744–4746.
- [75] Y. Wang, H. Zhang, G. Zhang, W. Tao, S. Tang, J. Lumin. 126 (2007) 211–218.
- [76] A. Wolfe, G. Shimer, T. Meehan, Biochemistry 26 (1987) 6392–6396.
- [77] M.T. Carter, M. Rodriguez, A.J. Bard, J. Am. Chem. Soc. 111 (1989) 8901–8911.
- [78] G. Zhao, H. Lin, S. Zhu, H. Sun, Y. Chen, J. Inorg. Biochem. 70 (1998) 219–226.
- [79] D.P. Heller, C.L. Greenstock, Biophys. Chem. 50 (1994) 305–312.
- [80] R.H. Blessing, Acta Crystallogr. Sect. A 51 (1995) 33–38.
- [81] A. Altomare, M.C. Burla, M. Camalli, G. Casciaro, C. Giacovazzo, A. Guagliardi, A.G. Moliterni, G. Polidori, R. Spagna, J. Appl. Crystallogr. 32 (1999) 115–119.
- [82] G.M. Sheldrick, SHELXTL Version 2014/7, in: <http://shelx.uni-ac.gwdg.de/SHELX/index.php>.
- [83] L.J. Farrugia, J. Appl. Crystallogr. 32 (1999) 837–838.
- [84] M.J. Frisch, G.W. Trucks, H.B. Schlegel, G.E. Scuseria, M.A. Robb, J.R. Cheeseman, G. Scalmani, V. Barone, B. Mennucci, G.A. Petersson, H. Nakatsuji, M. Caricato, X. Li, H.P. Hratchian, A.F. Izmaylov, J. Bloino, G. Zheng, J.L. Sonnenberg, M. Hada, M. Ehara, K. Toyota, R. Fukuda, J. Hasegawa, M. Ishida, T. Nakajima, Y. Honda, O. Kitao, H. Nakai, T. Vreven, J. Montgomery, J.E. Peralta, F. Ogliaro, M. Bearpark, J.J. Heyd, E. Brothers, K.N. Kudin, V.N. Staroverov, R. Kobayashi, J. Normand, K. Raghavachari, A. Rendell, J.C. Burant, S.S. Iyengar, J. Tomasi, M. Cossi, N. Rega, N.J. Millam, M. Klene, J.E. Knox, J.B. Cross, V. Bakken, C. Adamo, J. Jaramillo, R. Gomperts, R.E. Stratmann, O. Yazyev, A.J. Austin, R. Cammi, C. Pomelli, J.W. Ochterski, R.L. Martin, K. Morokuma, V.G. Zakrzewski, G.A. Voth, P. Salvador, J.J. Dannenberg, S. Dapprich, A.D. Daniels, Ö. Farkas, J.B. Foresman, J.V. Ortiz, J. Cioslowski, D.J. Fox, Revision A, 1st ed., Gaussian, Inc., Wallingford CT, 2009.
- [85] A.D. Becke, J. Chem. Phys. 98 (1993) 5648.
- [86] P.J. Stevens, F.J. Devlin, C.F. Chabowski, M.J. Frisch, J. Phys. Chem. 98 (1994) 11623–11627.
- [87] P.J. Hay, W.R. Wadt, J. Chem. Phys. 82 (1985) 270.
- [88] J. Tomasi, M. Persico, Chem. Rev. 94 (1994) 2027–2094.
- [89] M.N. Burnett, C.K. Johnson, ORTEP III. Report ORNL-6895, Oak Ridge National Laboratory, Oak Ridge, Tennessee, USA, 1996.
- [90] I. Ucar, O.Z. Yesilel, A. Bulut, H. Olmez, O. Buyukgungor, Acta Crystallogr. Sect. E 60 (2004) m1025.
- [91] K. Nakamoto, Infrared and Raman Spectra of Inorganic and Coordination Compounds, Part B: Applications in Coordination, Organometallic, and Bioinorganic Chemistry, sixth ed., Wiley, New Jersey, 2009.
- [92] N. Ahmad, A.H. Chughtai, H.A. Younus, F. Verpou, Coord. Chem. Rev. 280 (2014) 1–27.
- [93] R.P. Sharma, A. Singh, A. Saini, P. Venugopalan, A. Molinari, V. Ferretti, J. Mol. Struct. 923 (2009) 78–84.
- [94] R.P. Sharma, A. Saini, S. Singh, P. Venugopalan, W.T. Harrison, J. Fluor. Chem. 131 (2010) 456–460.
- [95] M.F. Khan, F.U. Rehman, G.M. Khan, I. Khan, Am. Lab. 41 (2009) 44–49.
- [96] M. Vicente, R. Bastida, A. Maci, L. Valencia, C. Gualdes, C.D. Brondino, Inorg. Chim. Acta 358 (2005) 1141.
- [97] B.J. Hathaway, A.A.G. Tomlinson, Coord. Chem. Rev. 5 (1970) 1–43.
- [98] V. Rajendiran, R. Karthik, M. Palaniandavar, H. Stoeckli-Evans, V.S. Periasamy, M.A. Akbarsha, B.S. Srinag, H. Krishnamurthy, Inorg. Chem. 46 (2007) 8208–8221.
- [99] Q. Zhang, J. Liu, H. Chao, G. Xue, L. Ji, J. Inorg. Biochem. 83 (2001) 49–55.
- [100] A.M. Pyle, J.P. Rehmann, R. Meshoyrer, C.V. Kumar, N.J. Turro, J.K. Barton, J. Am. Chem. Soc. 111 (1989) 3053–3063.
- [101] G. Prati, J. Bernadou, B. Meunier, Adv. Inorg. Chem. 45 (1998) 251–262.
- [102] A. Dimitrakopoulou, C. Dendrinou-Samara, A.A. Pantazaki, M. Alexiou, E. Nordlander, D.P. Kessissoglou, J. Inorg. Biochem. 102 (2008) 618–628.
- [103] J.L. Garcia-Gimenez, M. Gonzalez-Alvarez, M. Liu-Gonzalez, B. Macias, J. Borrás, G. Alzueta, J. Inorg. Biochem. 103 (2009) 923–934.
- [104] A. Patra, B. Sen, S. Sarkar, A. Pandey, E. Zangrando, P. Chattopadhyay, Polyhedron 51 (2013) 156–163.
- [105] W.D. Wilson, L. Ratmeyer, M. Zhao, L. Strekowski, D. Boykin, Biochemistry 32 (1993) 4098–4104.